# Kinetics of Salt-Induced J-aggregation of Cyanine Dyes

**Tatyana D. Slavnova and Alexander K. Chibisov**

*Center of Photochemistry, Russian Academy of Sciences, 119421 Moscow, Russia*

**Helmut Görner***

*Max-Planck-Institut für Bioanorganische Chemie, D-45413 Mülheim an der Ruhr, Germany*

*Received: January 12, 2005; In Final Form: March 18, 2005*

The addition of monovalent, divalent, and trivalent metal ions to three anionic ethyl *meso*-thiacarbocyanine dyes, an ethyl *meso*-oxacarbocyanine, and an imidacarbocyanine in aqueous solution at room temperature results in the production of J-aggregates within the range of tens to hundreds of seconds. The rate of formation of J-aggregates correlates with the rate of decay of dimers or monomers and is dependent on the type of metal ion, dye structure, and temperature. The rate of formation of J-aggregates increases as the temperature decreases and the dye and salt concentrations increase, and the rate is highest for trivalent ions and smallest for monovalent ions, independent of the type of anion. The time course of formation of J-aggregates is described in most cases by a sigmoidal curve, and the kinetics and mechanism are discussed within the framework of autocatalysis. Computer simulations reveal that the sigmoidal time dependence is transferred to an exponential-like curve by substantially increasing the rate constant for the noncatalytic step. The reaction pathway into J-aggregates can be switched from dimeric ion pairs as the reactant to monomeric ion pairs, when the rate constant for the catalytic step via the monomer becomes larger with respect to that via the dimer.

## Introduction

Cyanine dyes demonstrate a unique ability to form associates such as dimers and H- and J-aggregates.[1−5] The latter were originally discovered by Jelley and Scheibe.[1] Although the dimers are the simplest aggregates,[6−9] J-aggregates are representatives of polymer-type assemblies, which are composed of many thousands of dye monomers.[10−13] Primarily, the interest to study J-aggregates was based on their ability to sensitize AgHal photographic emulsions, where J-aggregates are formed upon adsorption onto AgHal microcrystals.[4,14] Recently, new applications of J-aggregates in electroluminescence[15−17] and nonlinear optical devices[18] were reported. This provides new impetus to study the properties of J-aggregates and to explore the mechanisms involved in their production.

J-aggregation was found to occur in aqueous solutions and water−methanol mixtures in the absence[8,19,20] and presence[3,20−25] of mostly monovalent metal ions, in the presence of surfactants,[20,26,27] polyelectrolytes,[28−31] polymers,[16,32] and Langmuir−Blodgett films.[30,33] J-aggregation is affected by the structure of cyanine dyes, where the presence of substituents in heterocyclic residues and the *N*-alkyl chain length influence the aggregation.[34−36] J-aggregates are characterized by unusual spectroscopic features, such as an extremely narrow and intense absorption band, as well as a small Stokes shift in fluorescence (almost resonance fluorescence). The properties could be simulated on the basis of one-dimensional molecular exciton models.[37−39]

In contrast to the great amount of data on J-aggregate properties in the excited and ground states, information regarding the kinetics of J-aggregation is limited to a few publications.[22,40−43] One reason for this is due to experimental difficulties in the measurement of the kinetics. J-aggregates are developed irregularly in solutions and result in a loss of homogeneity and the appearance of local turbidity, resulting in alterations of the light beam used to monitor the kinetics of aggregation by means of spectrophotometry. The kinetics of J-aggregation were mostly studied with 1,1′-diethyl-2,2′-cyanine iodide (PIC) in aqueous solution.[40−43] J-aggregation was observed to occur in the presence of relatively high concentrations of NaCl or $Na_2SO_4$, as well as on a polyvinylsulfonate template.[42,43] The results are described by "one-exponent" (first-order) kinetics[41] and are interpreted as a "simple" assembly of a self-similar fractal object.[43] Rather unusual was the observation of a negative temperature coefficient of J-aggregation for PIC.[40]

We have recently studied the kinetics of J-aggregation of anionic 3,3′-di($\gamma$-sulfopropyl)-5-methoxy-4′,5′-benzo-9-ethylthiacarbocyanine (**1**) in aqueous solution at room temperature.[22] The maximum rate of J-aggregation $(dA_J/dt)_{max}$ was shown to be nonlinearly dependent on dye concentration and strongly increase when going from monovalent (alkaline) metal ions to divalent (transition) and trivalent (rare-earth) metal ions, respectively. The formation of J-aggregates is described by a sigmoidal time course and was considered as an irreversible process. The kinetics and mechanism were rationalized in terms of autocatalysis.

In this paper, we extend the investigations of the kinetics of J-aggregation to two ethyl *meso*-thiacarbocyanine dyes (**2**, **3**), an ethyl *meso*-oxacarbocyanine (**4**), and an imidacarbocyanine (**5**) induced by the fast addition of certain monovalent, divalent, and trivalent metal ions, and we consider J-aggregation as a reversible process. We intend to clarify the role of metal ions and, in particular, their charges as the essential factor governing the rate of formation of J-aggregates as well as to ascertain if the rate is a nonlinear function of the dye concentration. Furthermore, we focus on the elucidation of the effect of the cyanine structure on the rate $dA_J/dt$. We also studied the effects of

* Author to whom correspondence should be addressed. E-mail: goerner@mpi-muelheim.mpg.de.

10.1021/jp058014k CCC: $30.25 
Published on Web 05/06/2005

temperature on the kinetics. A final objective is a detailed examination of the role of autocatalysis, possibly as a general mechanism for the J-aggregation of cyanine dyes.

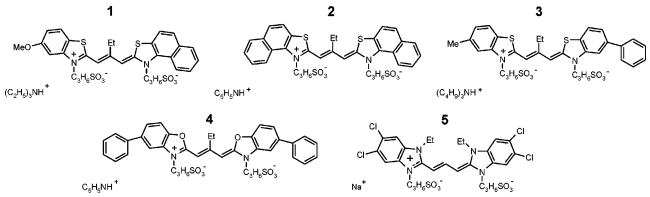


The principal results of this study are a nonlinear dependence of the rate of J-aggregation on the dye concentration and a strong dependence on the charge of metal ions. The negative temperature coefficient of J-aggregation for thiacarbocyanines and imidacarbocyanines reflects the effect of temperature on ion pairing and the dimer−monomer equilibrium. A sigmoidal time course for formation of most J-aggregates is a feature for the cyanines under study and can be treated within the framework of autocatalysis. Monomer and dimer ion pairs between dyes and metal ions are considered to serve as reactants for J-aggregation.

## Experimental Section

The thiacarbocyanines (**1**−**3**) were the same as those used previously,[7,9,22] and the oxacarbocyanine and imidacarbocyanine dyes (**4** and **5**) were a gift from Prof. Boris I. Shapiro of the Photographic Chemistry Institute in Moscow. Methanol and ethanol were spectroscopic grade, and water was obtained from a Milli Q system (Millipore). The solutions were freshly prepared by diluting from neat aqueous stock for **1**, **3**, and **4** (5−20 $\mu$M, pH 7), from methanol stock for **5**, and from ethanol stock for **2** (5−45 $\mu$M, pH 7, containing 1 vol % EtOH). Dye **5** is unstable in water; however, its stability was highly increased in a mixture of methanol and NaOH, as has been shown by Herz.[3] Thus, aqueous solutions of **5** (5−20 $\mu$M, pH 11) contained 1 mM NaOH and 7 M methanol. Trivalent ions for **5** were not used, because of possible interaction with $OH^-$, yielding hydroxide complexes. Either chlorides of $Na^+$ and $K^+$ ions or nitrates of $Mn^{2+}$, $Ni^{2+}$, $Eu^{3+}$, and $Tb^{3+}$ ions were used.[22] A diode array spectrophotometer (Hewlett−Packard model HP 8453) was used to measure absorption spectra at discrete time intervals (e.g., 4 s). A few microliters of solution of the appropriate salt concentration were injected into a 1-cm cell with the dye solution, followed by intense stirring for 1−2 s before starting the measurement. Further stirring was performed between each two consecutive runs. The rate of J-aggregation was evaluated from spectral data. Solving of the rate equations, the fitting procedure, and computer simulation were performed with Mathcad 2001. The derivative of the experimental curves was computed with Origin 5. The maximum J-aggregate concentration in the computer simulation was fitted using the maximum value of the absorbance of the J-band; i.e., we did not intend to estimate the absorption coefficient. The measurements refer to steady-state conditions in a (buffer-free) aqueous solution at 24 °C, unless otherwise indicated. Measurements at different temperatures were performed using a thermostat.

## Results

**J-aggregation Properties of Thiacarbocyanines and Oxacarbocyanine.** The absorption spectrum of thiacarbocyanine **2** (10 $\mu$M) in aqueous solution shows a short-wavelength maximum at 534 nm, which is assigned to the dimer (D-band), and a long-wavelength shoulder from the monomer (M-band) at $\lambda_M = 580$ nm. In the presence of $Mn(NO_3)_2$ (0.2 mM), a new band (J-band) with a maximum at $\lambda_J = 650$ nm appears, which is assigned to a J-aggregate. The formation of J-aggregates is accompanied by a decrease of the D-band and an isosbestic point at 562 nm (Figure 1). The time dependence of the absorbancies (kinetic curves) at 650 and 534 nm is characterized by the presence of both an induction period and an inflection point (see inset in Figure 1); the time (half-life of reaction, $t_{1/2}$) for the 50% value of the absorbance of the J-band ($A_J^{650}$) is 14 s. Formation of J-aggregates for **2** also occurs for KCl (4 mM) and $Ni(NO_3)_2$ at 0.2 mM, with $t_{1/2} = 10$ and 8 s, respectively. For all metal ions used as promoters of J-aggregation for **2**, an induction period is observed only at low dye and salt concentrations.

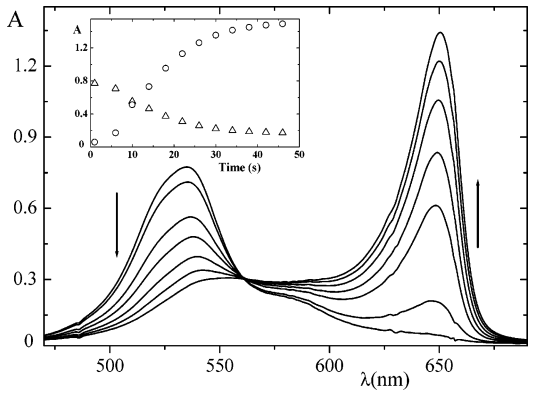


**Figure 1.** Absorption spectra of **2** (10 $\mu$M) in water at 24 °C in the presence of $Mn(NO_3)_2$ (0.2 mM), as a function of time. Inset shows the kinetics at (○) 650 nm and (△) 534 nm.

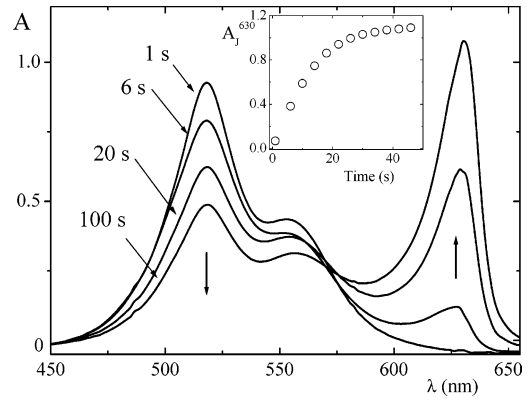


**Figure 2.** Absorption spectra of **3** (10 $\mu$M) in water at 24 °C in the presence of KCl (80 mM), as a function of time. Inset shows the kinetics at 630 nm.

To produce J-aggregates efficiently, a salt must be added. J-aggregation of **3** in the presence of KCl (80 mM) is characterized by absorption at three wavelengths: $\lambda_D = 518$ nm, $\lambda_M = 555$ nm, and $\lambda_J = 630$ nm. An example of the absorption spectra of **3** and KCl (80 mM), together with the corresponding time course, is presented in Figure 2. The kinetic curves of **3**, in contrast to **1** and **2**, exhibit neither an inflection point nor an induction period for monovalent, divalent, and trivalent metal ions. Moreover, the formation of J-aggregates is accompanied by a decrease of both D- and M-bands. The half-life is 8 s for $Mn(NO_3)_2$ and $Ni(NO_3)_2$ at 3 mM and 3 s for $Tb(NO_3)_3$ at 0.2 mM.

The ability to J-aggregate was also observed for oxacarbocyanine **4**. The spectrum of freshly prepared **4** (10−15 $\mu$M)

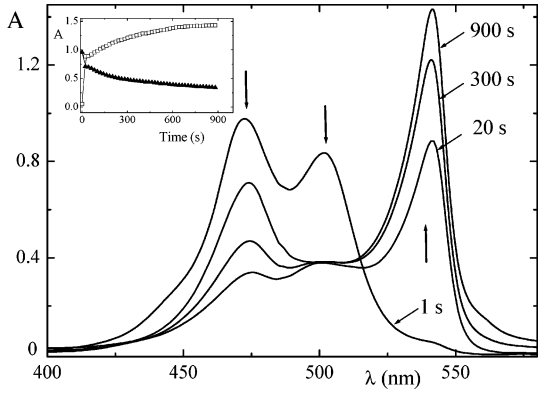


**Figure 3.** Absorption spectra of **4** (10 $\mu$M) in water at 24 °C in the presence of KCl (60 mM), as a function of time. Inset shows the kinetics at (▲) 475 nm and (○) 542 nm.

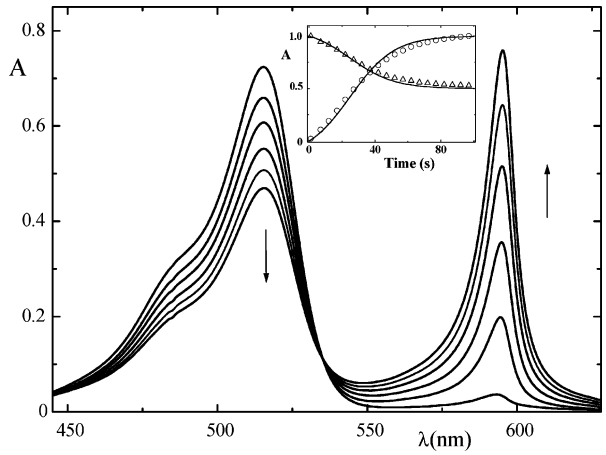


**Figure 4.** Absorption spectra of **5** (5 $\mu$M) in water at 24 °C in the presence of MeOH (7 M), NaOH (1 mM), and KCl (20 mM), as a function of time. Inset shows kinetic curves at (○) 595 nm and (△) 516 nm; curves have been fitted for $k_n = 5 \times 10^{-3}$ s$^{-1}$, $k_{-n} = 7 \times 10^{-2}$ s$^{-1}$, $k_c = 2.6 \times 10^4$ M$^{-1}$ s$^{-1}$, $K_1 = 50$ M$^{-1}$, and $n = 4$.

in water shows M-, D-, and J-bands at $\lambda_M = 472$ nm, $\lambda_D = 502$ nm, and $\lambda_J = 542$ nm, respectively. However, the absorbance $A_J$ disappears within 60 s, along with a simultaneous increase of the D-band. The subsequent addition of KCl (60 mM) results in fast formation of J-aggregates at the expense of the M- and D-bands, and an additional increase in $A_J$ at the expense of the dimer band (Figure 3). The kinetic curves for J-aggregation are sigmoidal ($t_{1/2} = 250$ s) with an induction period after the fast increase of $A_J$ (see inset in Figure 3). At a higher concentration of KCl (>80 mM), as well as when $Mn^{2+}$ (2 mM) or $Tb^{3+}$ (20 $\mu$M) are added, the J-band is formed instaneously and then decreases, whereas the D-band increases at the expense of the M- and J-bands.

**J-aggregation Properties of Imidacarbocyanine.** For **5** at 5 $\mu$M in aqueous solution mixed with methanol (7 M) and NaOH (1 mM), the absorption spectrum exhibits a short-wavelength maximum at $\lambda_m = 515$ nm but no dimer peak (Figure 4). The J-band with $\lambda_J = 595$ nm appears in the presence of KCl, $Ni(NO_3)_2$, or $Mn(NO_3)_2$. Formation of the J-band with $t_{1/2} = 27$, 47, and 30 s in the presence of KCl (20 mM), $Ni(NO_3)_2$, and $Mn(NO_3)_2$ at 0.2 mM, respectively, is accompanied by a decrease of the M-band and is manifested with the isosbestic point at 535 nm. The kinetic curves are sigmoidal, with a faintly discernible induction period.

The formation of J-aggregates is accompanied by a decrease of the M-band for **5** and a decrease of the D-band for **1**−**4**. It is noteworthy that a decrease of the D- and M-bands for **1**−**4** and **5**, respectively, and the increase of the J-band occurs only during a specific time. The absorbances of the D- and M-bands remain constant and are larger than zero (denoted as the remaining absorbance). Examples for the decrease of the M-band (Figure 4) and the D-band (Figure 5) are presented. The values of the remaining absorbance of the D- and M-bands, as well as the $A_J$ value, are dependent on the salt concentration, decreasing with increasing salt concentration for both D- and M-bands and increasing for the J-band.

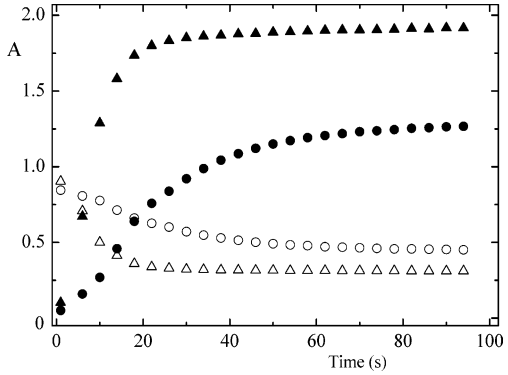


**Figure 5.** Kinetic curves of the decay of dimers (open symbols) and the formation of J-aggregates (closed symbols) for **1** (11 $\mu$M) in water in the presence of 50 mM KCl (circles) and 80 mM (triangles) KCl.

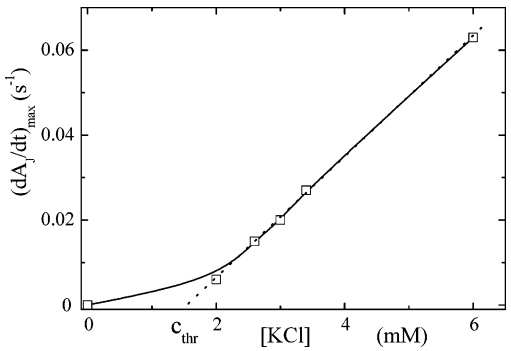


**Figure 6.** Dependence of $(dA_J/dt)_{max}$ on the concentration of KCl for **2** (8 $\mu$M) in water at 24 °C. Dotted line represents the extrapolation for $(dA_J/dt)_{max} = 0$, and $c_{thr}$ denotes the threshold salt concentration.

**Effects of Salt and Dye Concentrations.** For a quantative description of the effect of J-aggregation, the maximum rate, $(dA_J/dt)_{max}$, was used.[22] For systems where the kinetic curves of J-aggregation are sigmoidal, $(dA_J/dt)_{max}$ corresponds to the inflection point. For those systems, which exhibit a nonsigmoidal behavior, the $(dA_J/dt)_{max}$ value corresponds to the initial step of J-aggregation. Plots of $(dA_J/dt)_{max}$ versus the salt concentration are shown for **2** with KCl (see Figure 6) and for **1** with $MgCl_2$.[22] For **2** (40 $\mu$M) without salt, $(dA_J/dt)_{max} = 0.004$ s$^{-1}$ and ranges between 0.005 and 0.06 s$^{-1}$ in the presence of 2−6 mM KCl.

The J-aggregation starts to develop at a threshold salt concentration $c_{thr}$; at concentrations higher than $c_{thr}$, the rate $(dA_J/dt)_{max}$ shows a linear dependence (Figure 6). For **2**, **5**, and **1**, each in the presence of KCl, the $c_{thr}$ values are 1.5, 8, and 15 mM, respectively. We used the "normalized" rate of J-aggregation, denoted as $(dA_J/dt)_{max}/[M^{z+}]$, where $[M^{z+}]$ is the concentration of metal ion. The values are compiled in Table 1; for divalent ions, the values are in the range of 8−530 M$^{-1}$ s$^{-1}$. The effects are strikingly greater when a monovalent or divalent ion is replaced by a trivalent ion, where the values are between $2 \times 10^2$ M$^{-1}$ s$^{-1}$ and $10^5$ M$^{-1}$ s$^{-1}$.

The time dependences of the absorbance $A_J$ at different concentrations of **5**, in the presence of 10 mM KCl, are shown

**TABLE 1. Normalized Rate of J-aggregation, $(dA_J/dt)_{max}/[M^{z+}]$, for Various Cases[a]**

| | $(dA_J/dt)_{max}/[M^{z+}]$ ($M^{-1}$ $s^{-1}$) | | | | |
|---|---|---|---|---|---|
| cation | dye **1**[b] | dye **2** | dye **3** | dye **4** | dye **5** |
| $K^+$ | 0.3 | 15 | 0.4 | 0.01 | 8 |
| $Mn^{2+}$ | 12 | 340 | 12 | | 120 |
| $Ni^{2+}$ | 13 | 530 | 8 | | 65 |
| $Tb^{3+}$ | 10 000 | >10 000 | 210 | | *c* |

[a] At 24 °C, using a dye concentration of 10 $\mu$M. [b] Taken from ref 22. [c] Not possible with $Tb^{3+}$.

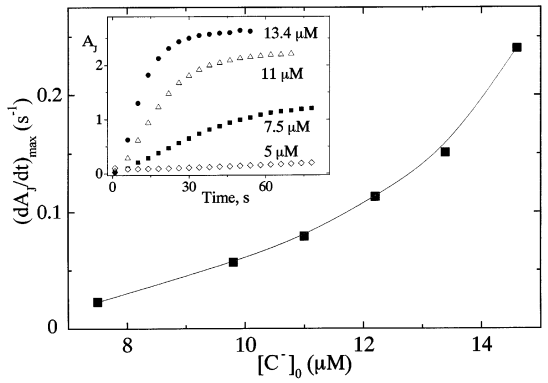


**Figure 7.** Dependence of $(dA_J/dt)_{max}$ on the total concentration of **5** in the presence of KCl (10 mM) in a mixture of water, methanol (7 M), and NaOH (1 mM) at 24 °C. Inset shows the kinetic curves of J-aggregation at 595 nm at different dye concentrations.

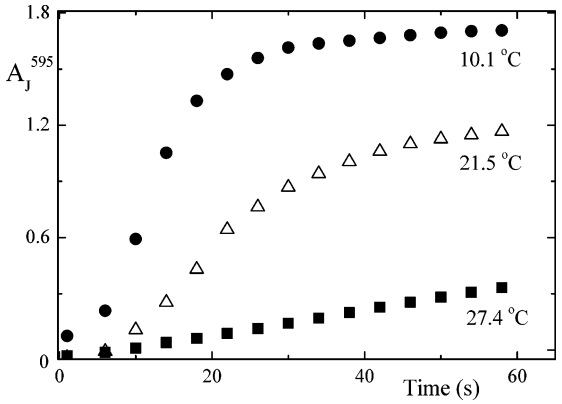


**Figure 8.** Kinetic curves of J-aggregation for **5** (6 $\mu$M) in the presence of KCl (16 mM) in a mixture of water, MeOH (7 M), and NaOH (1 mM) at different temperatures.

in Figure 7 (inset). The shape of the kinetic curves is strongly dependent on the total dye concentration ($[C^-]_0$), and the dependence of the rate of J-aggregation is curved upward (see Figure 7). The increase of [**5**], in the order of 7.5, 11.0, and 14.6 $\mu$M, results in a transformation of the sigmoidal-type curve into a nonsigmoidal curve and an enhancement of the $(dA_J/dt)_{max}$ value: 0.02, 0.08, and 0.24 $s^{-1}$, respectively.

**Effect of Temperature.** So far, the results have referred to room temperature. When the temperature is decreased, $(dA_J/dt)_{max}$ is increased. This is shown in Figure 8 for **5**, and similar kinetic curves were observed for **1**. The change in temperature, from 8 °C to 27 °C, results in variation of the rate by a factor of 3−5 (Table 2). The type of metal ion does not noticeably influence the temperature coefficient of J-aggregation, $\Delta(dA_J/dt)_{max}/\Delta T$. For **1**, the value is in the range of −0.001 to −0.002 (s °C)$^{-1}$ for $K^+$, $Mn^{2+}$, and $Tb^{3+}$ and the value is twofold more negative for **5** with KCl.

**TABLE 2. Values Obtained from Variation of the Temperature[a]**

| cation | temperature (°C) | $(dA_J/dt)_{max}$ ($s^{-1}$) |
|---|---|---|
| | Dye **1** | |
| $K^+$ | 24 | 0.01 |
| $K^+$ | 8.4 | 0.05 |
| $Mn^{2+}$ | 25.4 | 0.005 |
| $Mn^{2+}$ | 10.1 | 0.02 |
| $Tb^{3+}$ | 25 | 0.006 |
| $Tb^{3+}$ | 9.6 | 0.02 |
| | Dye **5**[b] | |
| $K^+$ | 27.4 | 0.007 |
| $K^+$ | 21.5 | 0.05 |
| $K^+$ | 10.1 | 0.1 |

[a] Using dye concentrations of [**1**] = 10 $\mu$M and [**5**] = 5.2 $\mu$M. [b] Using 7 M methanol and 1 mM NaOH.

## Discussion

Sigmoidal time dependences with an inflection point have been reported for the self-association of porphyrins[43,44] and bacteriochlorophyll,[45] the formation of transition-metal nanoclusters,[46] and the polymerization of proteins.[47] The kinetics were characterized by an induction period and treated within the framework of autocatalysis.[43,45,46] However, the sigmoidal build-up curves of a product P are also compatible with a consecutive reaction R → X → P. In this case, however, reactant R decays exponentially and no induction period is involved in the step R → X. Thus, an interpretation of the reaction mechanism should be based on the analysis of the kinetics of both the formation of P and the decay of R. For **1** in water, the kinetics of formation of J-aggregates as the product and the decay of the dimer as the reactant, in the presence of metal ions, were described by sigmoidal time dependences and considered as autocatalytic irreversible reactions.[22] The autocatalytic mechanism is illustrated in Scheme 1, where $k_n$ and $k_c$ are the rate constants for noncatalytic and catalytic production of product P, respectively.[22,48]

**SCHEME 1**

$$\mathrm{R} \xrightarrow{k_n + k_c[\mathrm{P}]} \mathrm{P}$$

Scheme 1 is adopted as a whole in the present study for all dyes. As follows from the results, the J-aggregation of the five dyes at concentrations of ~10 $\mu$M occurs only in the presence of metal ions. It is reasonable to assume that metal ions produce ion pairs with the dye, where the inherent counterion is replaced by the metal ion at an appropriate salt concentration. In particular, the replacement of triethylammonium as the counterion for **1** by $Na^+$ has been reported previously.[25]

**Reaction Scheme without Dimers.** Dye **5** is monomeric in the applied mixture with methanol and NaOH, and the ion pair is supposed to be formed between the monomer and the metal ion, where $K_1 = [C^-M^{z+}]/[C^-][M^{z+}]$.

$$C^- + M^{z+} \rightleftharpoons C^-M^{z+} \quad (1)$$

We suggest that the ion pair $C^-M^{z+}$ is the reactant and the product is obviously the J-aggregate. Forward reaction 1 is probably fast, as it has been reported for spiropyran-derived merocyanines.[49] As has been mentioned previously, dye **5** is not fully converted to J-aggregates. This follows from the M-band absorbance that remains after J-aggregation (see Figure 4). This observation implies that J-aggregation is a reversible

process, and, thus, Scheme 1 should be rearranged to Scheme 2, which includes the reverse step with the rate constant $k_{-n}$.

**SCHEME 2**

$$C^- + M^{z+} \overset{K_1}{\rightleftharpoons} C^-M^{z+} \underset{k_{-n}}{\overset{k_n + k_c[J]}{\rightleftharpoons}} J$$

We believe that a rapidly established equilibrium occurs during the formation of the J-aggregates; consequently, the concentrations of $C^-$ and $C^-M^{z+}$ are kept equilibrated. Also, the positions of the maxima of monomers and ion pairs in the absorption spectra coincide; so far, the absorbance of the M-band consists of that for monomers and ion pairs. Considering the formation of J-aggregates as a reversible reaction and using Scheme 2, the rate of J-aggregation is given as

$$\frac{d[J]}{dt} = (k_n + k_c[J])[C^-M^{z+}] - k_{-n}[J] \quad (2)$$

The relationship between the rate for decay of the ion pairs $C^-M^{z+}$ and monomers and that for the formation of J-aggregates is given by eqs 3 and 4 for $[M^{z+}] \gg [C^-]$.

$$-\frac{d[C^-M^{z+}]}{dt} = \left(\frac{nK_1[M^{z+}]}{1 + K_1[M^{z+}]}\right)\frac{d[J]}{dt} \quad (3)$$

$$-\frac{d[C^-]}{dt} = \left(\frac{n}{1 + K_1[M^{z+}]}\right)\frac{d[J]}{dt} \quad (4)$$

Here, $n$ is the number of monomers included in the J-aggregate. Solving eqs 2−4 yields the time dependences of the concentrations of J-aggregates, monomers, and ion pairs (see Appendix I). The plots of [J] versus time, as well as $[C^-] + [C^-M^{z+}]$ versus time, are sigmoidal-type curves, which are characterized by the presence of both induction period and inflection point (see Figure 9, curves 1 and 2). Shortening of the induction period due to increasing $k_n$ or decreasing $k_{-n}$ results in the transformation of the sigmoidal curve to a nonsigmoidal-type curve. The results of computer simulations for two $k_n$ values are presented in Figure 9, where the decay curves refer to the total concentration of monomers and ion pairs. Increasing either $[C^-]$ or $[M^{z+}]$ does not lead to a transformation of the sigmoidal curve to the nonsigmoidal curve.

The existence of the induction period is also characteristic for crystallization,[50] which requires the spontaneous formation of a "critical" aggregation nucleus. Accordingly, the rate constants $k_n$ and $k_{-n}$ describe the reversible process of nuclei formation, whereas $k_c$ characterizes the growth of J-aggregates as a result of the interaction of nuclei with ion pairs.

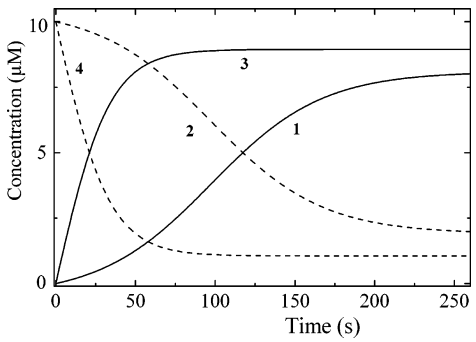


**Figure 9.** Computer simulations for the formation of J-aggregates (solid lines) and the decay of monomers and ion pairs ($[C^-] + [C^-M^{z+}]$) (dashed lines) for $[C^-]_0 = 10\ \mu M$, $K_1 = 1 \times 10^2\ M^{-1}$, $[M^{z+}] = 10$ mM, $k_c = 1 \times 10^4\ M^{-1}\ s^{-1}$, $k_n = 0.001\ s^{-1}$ (for **1**, **2**) and $k_n = 0.02\ s^{-1}$ (for **3**, **4**); $k_{-n} = 0.01\ s^{-1}$, $n = 4$.

Taking into account that $\lambda_J$ is invariant in the course of J-aggregation, the presence of isosbestic points in absorption spectra for the dyes under study would suggest that the number of monomers included in J-aggregates and responsible for J-aggregate absorbance remains constant. This was also confirmed by the spectroscopic observation of the constancy of the aggregation number for **5**[3] and relative dyes[20,51] at different concentrations. It implies that the changes in absorbance used for description of the kinetics in time-resolved spectroscopic measurements is proportional to the changes in the concentration of J-aggregates. It is noteworthy that both the nuclei and J-aggregates are characterized by similar absorption and cannot be distinguished. The applicability of the model used to describe the kinetics of both the formation of J-aggregates and decay of monomers/monomeric ion pairs follows from the agreement between the experimental data and results from the fitting procedure. Figure 4 (inset) shows the results of the curve-fitting for **5** in the presence of 20 mM KCl, which implies, in particular, that $k_n$ is smaller than $k_{-n}$.

**Reaction Scheme with Dimers.** In contrast to dye **5**, dyes **1**−**4** are present in water as an equilibrated mixture of monomers and dimers ($C_2^{2-}$), where $K_2 = [C_2^{2-}]/[C^-]^2$.

$$2C^- \rightleftharpoons C_2^{2-} \quad (5)$$

The dimers can also form ion pairs $C_2^{2-}M^{z+}$ which might be even more favorable due to the higher negative charge on the dimer with respect to the monomer, where $K_3 = [C_2^{2-}M^{z+}]/([C_2^{2-}][M^{z+}])$.

$$C_2^{2-} + M^{z+} \rightleftharpoons C_2^{2-}M^{z+} \quad (6)$$

For dyes **1**−**4**, we propose Scheme 3, where the ion pairs $C^-M^{z+}$ and $C_2^{2-}M^{z+}$ are the reactants and $k_{dn}$ and $k_{dc}$ are the rate constants for noncatalytic and catalytic J-aggregate production from dimer ion pairs, respectively, and $k_{-dn}$ refers to the back step. Considering the possible equilibrium between the two ion pairs in Scheme 3, we have omitted it, for the sake of simplicity.

**SCHEME 3**

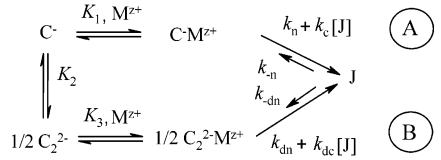


Generally, the formation of J-aggregates proceeds via reaction pathways A and B in Scheme 3. For some specific conditions, either pathway A or B can dominate. It is difficult to distinguish between both pathways, because of the lack of the data on the rate and equilibrium constants. We used a computer simulation that took the mass balance law (eq 7) into consideration to predict the most favorable pathway of J-aggregation:

$$[C^-] + [C^-M^{z+}] + 2[C_2^{2-}] + 2[C_2^{2-}M^{z+}] + n[J] = [C^-]_0 \quad (7)$$

The rate equations described by eqs 8−12, which describe the kinetics of J-aggregation and the decay of ion pairs $C^-M^{z+}$, $C_2^{2-}M^{z+}$, monomers $C^-$, and dimers $C_2^{2-}$ are given in Appendix II. Analytical solution of the rate equations to determine $[J](t)$, $[C^-M^{z+}](t)$, $[C^-](t)$, $[C_2^{2-}](t)$, and $[C_2^{2-}M^{z+}](t)$ could not be achieved; however, eqs 8−12 were solved numerically, and

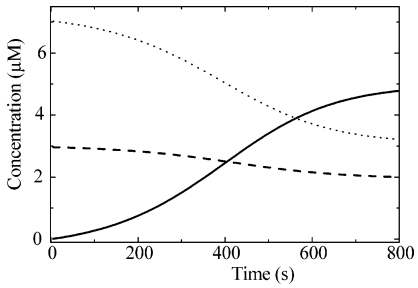


**Figure 10.** Computer simulations for the formation of J-aggregates (solid line) and the decay of monomers and ion pairs ($[C^-] + [C^-M^{z+}]$) (dashed line) and dimers and ion pairs ($[C_2^{2-}] + [C_2^{2-}M^{z+}]$ (dotted line) for $[C^-]_0 = 10\ \mu M$, $[M^{z+}] = 10$ mM, $k_c = k_{dc} = 1 \times 10^4\ M^{-1}\ s^{-1}$, $k_n = k_{dn} = 0.001\ s^{-1}$, $k_{-n} = k_{-dn} = 0.01\ s^{-1}$; $K_1 = 1 \times 10^2\ M^{-1}$, $K_2 = 2 \times 10^5\ M^{-1}$, and $K_3 = 1.5 \times 10^3\ M^{-1}$ for pathway A in Scheme 3.

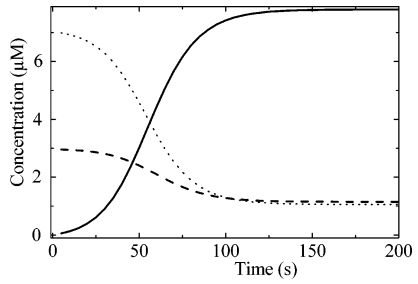


**Figure 11.** Computer simulations for the formation of J-aggregates (solid line) and the decay of monomers and ion pairs ($[C^-] + [C^-M^{z+}]$) (dashed line) and dimers and ion pairs ($[C_2^{2-}] + [C_2^{2-}M^{z+}]$ (dotted line) for $[C^-]_0 = 10\ \mu M$, $[M^{z+}] = 10$ mM, $k_c = k_{dc} = 1 \times 10^4\ M^{-1}\ s^{-1}$, $k_n = k_{dn} = 0.001\ s^{-1}$, $k_{-n} = k_{-dn} = 0.01\ s^{-1}$; $K_1 = 1.5 \times 10^3\ M^{-1}$, $K_2 = 2 \times 10^5\ M^{-1}$, and $K_3 = 1 \times 10^2\ M^{-1}$ for pathway B in Scheme 3.

Figures 10 and 11 show the results for separated pathways A and B, respectively. To choose the appropriate parameters, we explored a qualitative agreement between calculated and experimental kinetic curves. For simplicity, we assumed that $k_n = k_{dn}$ and $k_{-n} = k_{-dn}$, where $k_n$ and $k_{dn}$ are responsible for the induction period, whereas $k_{-n}$ and $k_{-dn}$ are responsible for the remaining absorbance. The value $K_2 = 2 \times 10^5\ M^{-1}$ characterizes the dimerization of thiacarbocyanine dyes,[6] whereas the relation $K_3 \gg K_1$ is a consequence of the experimental result that the D-band is 2−3 times higher than the M-band. The absorption spectra of free monomers and their ion pairs were assumed to be similar, and the same was adopted for free dimers and their ion pairs, respectively. The assumption is based on the constancy of the shape of the absorption spectra immediately after the addition of salts to **1**−**3**.

From the kinetic curves computed for both pathways and presented in Figures 10 and 11, it follows that the curves for the formation of J-aggregates and decay of dimers and ion pairs are sigmoidal and characterized by an induction period and an inflection point. On the basis of computer simulations, we found that the sigmoidal curve is transformed to a nonsigmoidal curve when the rate constants $k_n$ and $k_{dn}$, which govern nucleus formation, increase (not shown). **1** and **2** exhibit sigmoidal curves for monovalent, divalent, and trivalent metal ions at appropriate dye and salt concentrations, which are transformed to a nonsigmoidal curve, e.g., at higher salt concentration (Figure 5). Thus, a noncatalytic process actually follows pseudo-first-order kinetics and the rate constant is a product of the rate constant of ion-pair stacking and the ion-pair concentration. This is confirmed by the observation of a threshold salt concentration in the kinetics of J-aggregation (see Figure 6). Thus, the formation of the nucleus can be considered to be the sequence of the reversible stacking steps, which is finished by the production of a "critical" aggregation nucleus (small J-aggregates). The sigmoidal−nonsigmoidal transformation also occurs when the dye concentration is increased. This is shown in Figure 7 (inset) for **5** and has been observed for bacteriochlorophyll.[45]

In contrast to **1** and **2**, nonsigmoidal curves were observed for **3** (see Figure 2) and were considered to be a result of transformation of the sigmoidal curve. The lack of an induction period and the nonsigmoidal kinetics have been reported for PIC in water[41] and in the presence of polyvinylsulfonate as a template.[43]

From a comparison of Figures 10 and 11, it follows that pathway B is more favorable and can be switched to pathway A, provided that $k_c \gg k_{dc}$. Generally, the rate constants $k_n$, $k_{-n}$, and $k_c$, which influence pathway A, can be different from the respective rate constants that govern pathway B. Therefore, the branching ratio between routes A and B is dependent mostly on the dye structure. Thus, we conclude that dyes with relatively fast kinetics of J-aggregation follow pathway B, whereas dyes with comparatively slow kinetics follow pathway A. Adopting this argument as the main reason for the difference between the two pathways, and taking into account that the half-lives in the presence KCl are $t_{1/2} = 28$, 4, 8, and 250 s for **1**, **2**, **3**, and **4**, respectively, one can suggest that **1**−**3** are involved in J-aggregation with dimeric ion pairs as the reactant, in contrast to **4**, which aggregates with monomeric ion pairs. This is supported by the data on the normalized rate of J-aggregation with KCl (see Table 1).

The absorbance of the D- and M-bands should be decreased in the course of J-aggregation, in accordance with Scheme 3. In fact, this is the case for **3** (see Figure 2). Moreover, the results of computer simulations predict only slight changes of the M-band absorbance in the course of J-aggregation via pathway A (see Figure 10).

From the data previously considered, one can see that there is an effect of dye structure on the kinetics and the J-aggregation pathway. A dye with highly hydrophobic properties (e.g., dye **2** at 40 $\mu$M) is able to aggregate to a certain extent, even without metal ions. Metal ions in aqueous solution strongly promote J-aggregation (not shown). Thiacarbocyanines **1** and **3** with moderate hydrophobic properties have the ability to J-aggregate only in the presence of metal ions. It is reasonable to suggest that dimeric ion pairs are the reactants in J-aggregation. In contrast to thiacarbocyanines **1**−**3**, J-aggregates of oxacarbocyanine **4** deaggregate in the presence of KCl (>80 mM), as well as $Mn(NO_3)_2$ (2 mM) and $Tb(NO_3)_3$ (20 $\mu$M), because of the competing formation of dimers and dimeric ion pairs. This confirms our suggestion that J-aggregation of imidacarbocyanine **5** proceeds via pathway A.

**Effects of Salt Concentration on the Aggregation Properties.** The normalized rate of J-aggregation of **1** with $Mg^{2+}$ is 23 $M^{-1}\ s^{-1}$, and this parameter was determined to be independent of the type of anion ($ClO_4^-$, $Cl^-$, or $NO_3^-$).[22] Inorganic salts, containing monovalent, divalent, and trivalent metal ions, are additives to promote J-aggregation. For **2** in the presence of 2 mM KCl, the $(dA_J/dt)_{max}$ value is enhanced 10-fold. The specificity of metal ions to influence the rate was taken into account by the normalized rate, $(dA_J/dt)_{max}/[M^{z+}]$. This is justified by the linear portion of the plot of $(dA_J/dt)_{max}$ versus salt concentration. The value of $(dA_J/dt)_{max}/[M^{z+}]$ was determined to be 0.01 $M^{-1}\ s^{-1}$ for **4** and 15 $M^{-1}\ s^{-1}$ for **2** in the case of KCl and between these two values for the other dyes

(see Table 1). Increasing of the rate of J-aggregation, when passing from monovalent to divalent and trivalent metal ions, can probably be explained by the ability of divalent and trivalent metal ions to coordinate more than one dye molecule, thus facilitating nucleus formation.

For **5**, the rate is also much faster with divalent ions than monovalent ions (see Table 1). We should emphasize that $(dA_J/dt)_{max}$ was generally determined to be independent of the type of anion constituting the salts,[22] and, thus, only metal cations have a crucial role in J-aggregation. The specificity of metal ions used is not only to affect the rate but also to increase the equilibrated concentration of J-aggregates at the time when the equilibrium is reached (see Figure 5). The reversibility of the J-aggregation process is confirmed by the observation of the remaining absorbance of the M- or D-bands (see Figures 4 and 5).

**Effects of Temperature on the Aggregation Properties.** For **1** and **5**, the temperature coefficient of J-aggregation, $\Delta(dA_J/dt)_{max}/\Delta T$, is negative (see results). A decrease of the rate with increasing temperature is unusual at first glance but has been reported for PIC[40] and bacteriochlorophyll.[45] The effect was interpreted by a decay of the nucleus at higher temperatures.[40] Considering nucleation as a reversible and spontaneous process (see Schemes 2 and 3), it is reasonable to expect the rate of J-aggregation to decrease with increasing temperature. Another possible explanation is a decrease of the concentration of the ion pairs, because of their dissociation into free monomers, when the temperature is increased. The effect is quite reasonable not only for the monomers of **5**, but also for other dyes, which are present as a mixture of monomers and dimers, where the latter form ion pairs as a reactant for J-aggregation. At higher temperatures, the competing equilibria (reactions 1, 5, and 6) are shifted toward the monomer, resulting in a negative temperature coefficient.

## Conclusion

The salt-induced J-aggregation of three ethyl *meso*-thiacarbocyanine dyes, an ethyl *meso*-oxacarbocyanine, and an imidacarbocyanine is a reversible autocatalytic reaction. Ion pairs between monomeric or/and dimeric dyes and metal ions in aqueous solution serve as reactants. The rate of J-aggregation is dependent nonlinearly on the dye concentration, is strongly influenced by the charge of the metal ions, and is independent of the type of anion constituting the salt. The kinetics are sigmoidal for most systems, whereas a nonsigmoidal curve is the result of a fast nucleation step, as a prerequisite of J-aggregation. The rate of aggregation is governed by the ion-pair concentration, which is influenced by the type of metal ions and temperature. At elevated temperatures, the rate is decreased, as a result of decreasing the ion-pair concentration and decay of the nuclei.

**Acknowledgment.** We thank Professor Wolfgang Lubitz for his support, Professor Boris I. Shapiro (of the Photographic Chemistry Institute, Moscow), for kindly providing dyes **4** and **5**, Professor Nikita A. Slavnov for handling the rate equations, and Mr. Leslie J. Currell for technical assistance. A.K.C. is grateful to the Deutsche Forschungsgemeinschaft and the Russian Fund for Basic Researches (No. 03-03-32931) for financial support.

## Appendix I

From mass balance, eq A1,

$$[C^-] + [C^-M^{z+}] + n[J] = [C^-]_0 \quad \text{(A1)}$$

equilibrium reaction 1, and eq 2, it follows that

$$-\frac{d[C^-]}{dt} = -\frac{k_c}{\alpha}(a^2[C^-]^2 - b[C^-] + q_{00}[C^-]_0) \quad \text{(A2)}$$

$$-\frac{d[C^-M^{z+}]}{dt} = -\frac{k_c}{a^2}(a^2[C^-M^{z+}]^2 - (\alpha-1)b[C^-M^{z+}] + (\alpha-1)^2 q_{00}[C^-]_0) \quad \text{(A3)}$$

$$\frac{d[J]}{dt} = -\beta k_c(n[J]^2 + p[J] - q_0[C^-]_0) \quad \text{(A4)}$$

Here,

$$\alpha = 1 + K_1[M^{z+}]$$

$$\beta = \frac{\alpha - 1}{\alpha}$$

$$a = \sqrt{\alpha(\alpha-1)}$$

$$q_0 = \frac{k_n}{k_c}$$

$$q_{00} = \frac{k_{-n}}{k_c}$$

$$b = (\alpha-1)nq_0 + (\alpha-1)[C^-]_0 + \alpha q_{00}$$

$$p = \left(\frac{q_{00}}{\beta}\right) + nq_0 - [C^-]_0$$

Integrating eqs A2 and A3 affords $[C^-](t)$ and $[C^-M^{z+}](t)$:

$$[C^-](t) = \frac{r - s\exp(\gamma t - Q)}{1 - \exp(\gamma t - Q)}$$

$$[C^-M^{z+}](t) = (\alpha-1)[C^-](t)$$

Here,

$$\gamma = 2k_c\sqrt{\beta}\sqrt{\frac{b^2}{4a^2} - q_{00}[C^-]_0}$$

$$Q = \ln\left(\frac{C_0 - r}{C_0 - s}\right)$$

$$C_0 = \frac{[C^-]_0}{\alpha}$$

$$r = \frac{b}{2a^2} - \frac{1}{a}\sqrt{\frac{b^2}{4a^2} - q_{00}[C^-]_0}$$

$$s = \frac{b}{2a^2} + \frac{1}{a}\sqrt{\frac{b^2}{4a^2} - q_{00}[C^-]_0}$$

Integrating eq A4 affords $[J](t)$:

$$[J](t) = \frac{\exp(\sigma t - B) - \upsilon}{\exp(\sigma t - B) + 1}$$

where

$$\sigma = 2k_c n\beta\sqrt{\frac{p^2}{4n^2} + \frac{[C^-]_0 q_0}{n}}$$

$$v = \frac{p}{2n} + \sqrt{\frac{p^2}{4n^2} + \frac{[C^-]_0 q_0}{n}}$$

$$\omega = -\frac{p}{2n} + \sqrt{\frac{p^2}{4n^2} + \frac{[C^-]_0 q_0}{n}}$$

$$B = \ln\left(\frac{\omega}{v}\right)$$

## Appendix II

The rate equations that describe the kinetics of J-aggregation and the decay of monomeric ion pairs, monomers, dimers, and dimeric ion pairs (see Scheme 3) are given as follows:

$$\frac{d[J]}{dt} = (k_n + k_c[J])[C^-M^{z+}] + (k_{dn} + k_{dc}[J])[C_2^{2-}M^{z+}] - (k_{-n} + k_{-dn})[J] \quad (8)$$

$$-\frac{d[C^-M^{z+}]}{dt} = \left(\frac{nK_1[M^{z+}]}{A}\right)\frac{d[J]}{dt} \quad (9)$$

$$-\frac{d[C^-]}{dt} = \left(\frac{n}{A}\right)\frac{d[J]}{dt} \quad (10)$$

$$-\frac{d[C_2^{2-}]}{dt} = \left(\frac{2nK_2[C^-]}{A}\right)\frac{d[J]}{dt} \quad (11)$$

$$-\frac{d[C_2^{2-}M^{z+}]}{dt} = \left(\frac{2nK_2K_3[M^{z+}][C^-]}{A}\right)\frac{d[J]}{dt} \quad (12)$$

Here, $A = 1 + K_1[M^{z+}] + 4K_2(1 + K_3[M^{z+}])[C^-]$.

## References and Notes


(1) (a) Scheibe, G. *Angew. Chem.* **1936**, *49*, 563. (b) Jelley, E. E. *Nature* **1936**, *138*, 1009.

(2) Sturmer, D. M.; Heseltine, D. W. In *The Theory of the Photographic Processes*, 4th Edition; James, T. H., Ed.; Macmillan: New York, 1977; p 194.

(3) Herz, A. H. *Photogr. Sci. Eng.* **1974**, *18*, 323.

(4) Shapiro, B. I. *Usp. Khim.* **1994**, *63*, 243. (English translation in *Russ. Chem. Rev.* **1994**, *63*, 231.)

(5) Mishra, A.; Behera, R. K.; Behera, P. K.; Mishra, B. K.; Behera, G. B. *Chem. Rev.* **2000**, *100*, 1973.

(6) Kopainsky, B.; Hallermeier, J. K.; Kaiser, W. *Chem. Phys. Lett.* **1981**, *83*, 498.

(7) Chibisov, A. K.; Zakharova, G. V.; Görner, H. *Phys. Chem. Chem. Phys.* **1999**, *1*, 1455.

(8) Chibisov, A. K.; Zakharova, G. V.; Görner, H. *Phys. Chem. Chem. Phys.* **2001**, *3*, 44.

(9) Chibisov, A. K.; Slavnova, T. D.; Görner, H. *Chem. Phys. Lett.* **2004**, *386*, 301.

(10) Scheblykin, I. G.; Varnavsky, O. P.; Bataiev, M. M.; Sliusarenko, O.; Van der Auweraer, M.; Vitukhnovsky, A. G. *Chem. Phys. Lett.* **1988**, *298*, 341.

(11) Sundström, V.; Gillbro, T.; Gadonas, R. A.; Piskarskas, A. *J. Chem. Phys.* **1988**, *89*, 2754.

(12) von Berlepsch, H.; Böttcher, C.; Ouart, A.; Burger, C.; Dähne, S.; Kirstein, S. *J. Phys. Chem. B* **2000**, *104*, 5255.

(13) Weigand, R.; Rotermund, F.; Penzkofer, A. *Chem. Phys.* **1997**, *220*, 3273.

(14) (a) West, W.; Gilman, P. B. In *The Theory of the Photographic Processes*, 4th Edition; James, T. H., Ed.; Macmillan: New York, 1977; p 251. (b) Carroll, B. H.; Higgins, G. C.; James, T. H. *Introduction to Photographic Theory. The Silver Halide Process*; Wiley: New York, 1980.

(15) Mal'tsev, I.; Lypenko, D. A.; Shapiro, B. I.; Brusentseva, M. A.; Milburn, G. H. W.; Wright, J.; A. Hendriksen, A.; Berendyaev, V. I.; Kotov, B. V.; Vannikov, A. V. *Appl. Phys. Lett.* **1999**, *75*, 1896.

(16) Scheblykin, I. G.; Lepnev, L. S.; Vitukhnovsky, A. G.; Van der Auweraer, M. *J. Lumin.* **2001**, *94*−*95*, 461.

(17) Bourbon, S.; Gao, M. Y.; Kirstein, S. *Synth. Met.* **1999**, *101*, 152.

(18) Sasaki, F.; Kobayashi, S. *J. Lumin.* **1997**, *72*−*74*, 538.

(19) (a) Rotermund, F.; Weigand, R.; Penzkofer, A. *Chem. Phys.* **1997**, *220*, 385. (b) Mauerer, M.; Penzkofer, A.; Zweck, J. *J. Photochem. Photobiol., B: Biol.* **1998**, *47*, 68. (c) Moll, J.; Daehne, S.; Durrant, J. R.; Wiersma, D. A. *J. Chem. Phys.* **1995**, *102*, 6362. (d) Lindrum, M.; Glismann, A.; Moll, J.; Daehne, S. *Chem. Phys.* **1993**, *178*, 423. (e) Johnson, A. E.; Kumazaki, S.; Yoshihara, K. *Chem. Phys. Lett.* **1993**, *211*, 511. (f) Zweck, J.; Penzkofer, A. *Chem. Phys.*, **2001**, *269*, 399. (g) He, P. S.; Zhou, X. F.; Peng, Z. H.; Geise, H. J. *J. Imag. Sci. Technol.* **1995**, *39*, 257.

(20) Daltrozzo, E.; Scheibe, G.; Gschwind, K.; Haimerl, F. *Photogr. Sci. Eng.* **1974**, *18*, 441.

(21) Struganova, I. A.; Lim, H.; Morgan, S. A. *J. Phys. Chem. B* **2002**, *106*, 11047.

(22) Chibisov, A. K.; Görner, H.; Slavnova, T. D. *Chem. Phys. Lett.* **2004**, *390*, 240.

(23) Ikegami, K. *Chem. Phys. Lett.* **2004**, *401*, 590.

(24) Chibisov, A. K.; Görner, H.; Slavnova, T. D. *Chem. Phys. Lett.* **2004**, *401*, 592.

(25) Xiang, J.; Yang, X.; Chen, C.; Tang, Y.; Yan, W.; Xu, G. *J. Colloid Interface Sci.* **2003**, *258*, 198.

(26) Chibisov, A. K.; Prokhorenko, V. I.; Görner, H. *Chem. Phys.* **1999**, *250*, 47.

(27) Tatikolov, A. S.; Costa, S. M. B. *Chem. Phys. Lett.* **2001**, *346*, 233.

(28) Peyratout, C.; Donath, E.; Daehne, L. *Photochem. Photobiol. Sci.* **2002**, *1*, 87.

(29) Liu, M.; Kira, A. *Thin Solid Films* **2000**, *359*, 104.

(30) Fukumoto, H.; Yonezawa, Y. *Thin Solid Films* **1998**, *327*, 748.

(31) Rousseau, E.; Koetse, M. M.; Van der Auweraer, M.; De Schryver, F. C. *Photochem. Photobiol. Sci.* **2002**, *1*, 395.

(32) (a) Higgins, D. A.; Barbara, P. F. *J. Phys. Chem.* **1995**, *99*, 3. (b) Misawa, K.; Ono, H.; Minoshima, K.; Kobayashi, T. *Appl. Phys. Lett.* **1993**, *63*, 577. (c) Misawa, K.; Ono, H.; Minoshima, K.; Kobayashi, T. *J. Lumin.* **1994**, *60*, 809. (d) Horng, M.-L.; Quitevis, E. L. *J. Phys. Chem.* **1993**, *97*, 12408. (e) Vacha, M.; Hashizume, K.-I.; Tani, T. *J. Lumin.* **2000**, *87*−*89*, 730. (f) Zakharova, G. V.; Kombaev, A. P.; Chibisov, A. K.; *Khim. Vysok. Energ.* **2004**, *38*, 211. (English translation in *High Energy Chem.* **2004**, *38*, 180.)

(33) Ishizawa, H.; Sato, T.; Sluch, M. I.; Vitukhnovsky, A. G. *Thin Solid Films* **1996**, *285*, 134.

(34) Tachibana, H.; Sato, F.; Terrettaz, S.; Azumi, R.; Nakamura, T.; Sakai, H.; Abe, M.; Matsumoto, M. *Thin Solid Films* **1998**, *327*−*329*, 813.

(35) Rousseau, E.; Van der Auweraer, M.; De Schryver, F. C. *Langmuir* **2000**, *16*, 8865.

(36) De Rossi, U.; Moll, J.; Spieles, M.; Bach, G.; Dähne, S. *J. Prakt. Chem.* **1995**, *337*, 203.

(37) De Rossi, U.; Moll, J.; Kriwanek, J.; Daehne, S. *J. Fluoresc.* **1994**, *4*, 53.

(38) Avdeeva, V. I.; Shapiro, B. I. *Sci. Appl. Photo.* **1998**, *39*, 543.

(39) (a) Davydov, A. S. *Theory of Molecular Excitons*; Plenum Press: New York, 1971. (b) Knoester, J. *J. Chem. Phys.* **1993**, *99*, 8466. (c) Kasha, M. *Radiat. Res.* **1963**, *20*, 55.

(40) Tanaka, T.; Iwasaki, M. *J. Imag. Sci.* **1989**, *33*, 78.

(41) Struganova, I. *J. Phys. Chem. A* **2000**, *104*, 9670.

(42) Struganova, I. A.; Hazell, M.; Gaitor, J.; McNally-Carr, D.; Zivanovic, S. *J. Phys. Chem. A* **2003**, *107*, 2650.

(43) Pasternack, R. F.; Fleming, C.; Herring, S.; Collings, P. J.; dePaula, J.; DeCastro, G.; Gibbs, E. J. *Biophys. J.* **2000**, *79*, 550.

(44) Pasternack, R. F.; Gibbs, E. J.; Collings, P. J.; dePaula, J. C.; Turzo, L. C.; Terracina, A. *J. Am. Chem. Soc.* **1998**, *120*, 5873.

(45) Balaban, T. D.; Leitich, J.; Holzwarth, A. R.; Schaffner, K. *J. Phys. Chem. B* **2000**, *104*, 1362.

(46) Watzky, M. A.; Finke, R. G. *J. Am. Chem. Soc.* **1997**, *119*, 10382.

(47) Kodaka, M. *Biophys. Chem.* **2004**, *109*, 325.

(48) Schmidt, R.; Sapunov, V. N. *Nonformal Kinetics*; Verlag Chemie: Weinheim, Germany, 1982.

(49) Chibisov, A. K.; Görner, H. *Chem. Phys.* **1998**, *237*, 425.

(50) Oxtoby, D. W. *Acc. Chem. Res.* **1998**, *31*, 91.

(51) Tanaka, T.; Matsubara, T. *J. Imag. Sci.* **1993**, *37*, 585.